The Tyrosine Kinase $p60^{c\text{-}src}$ Regulates the Fast Gate of the Cystic Fibrosis Transmembrane Conductance Regulator Chloride Channel

Horst Fischer and Terry E. Machen
University of California, Department of Molecular and Cell Biology, Division of Cell and Developmental Biology, Berkeley, California 94720-3200 USA

ABSTRACT The role of the tyrosine kinase $p60^{c\text{-}src}$ on the gating of the cystic fibrosis transmembrane conductance regulator (CFTR) chloride channel was investigated with the cell-attached and excised patch clamp technique in conjunction with current noise analysis of recordings containing multiple channels per patch. Spectra of CFTR-generated current noise contained a low-frequency and a high-frequency Lorentzian noise component. In the cell-attached mode, the high-frequency Lorentzian was significantly dependent on the membrane potential, while the low-frequency Lorentzian was unaffected. Excision of forskolin-stimulated patches into ATP-containing solution significantly reduced the amplitude of the voltage-dependent high-frequency Lorentzian. Addition of the tyrosine kinase $p60^{c\text{-}src}$ to excised, active, CFTR-containing membrane patches increased mean currents by 54%, increased the corner frequency of the low-frequency Lorentzian, and recovered the high-frequency Lorentzian and its characteristics. Treatment with lambda-phosphatase inactivated src-induced currents and changes in gating. When active patches were excised under conditions in which patch-associated tyrosine phosphatases were blocked with sodium vanadate, the high-frequency gating remained relatively unchanged. The results suggest that CFTR's open probability and its voltage-dependent fast gate are dependent on tyrosine phosphorylation, and that membrane-associated tyrosine phosphatases are responsible for inactivation of the fast gate after patch excision.

INTRODUCTION

The autosomal recessive inherited disease cystic fibrosis is caused by mutations in the gene coding for the cystic fibrosis transmembrane conductance regulator (CFTR) chloride channel. A whole array of described mutations lead to both dysfunctional and misprocessed channels (Tsui, 1992). CFTR is the major epithelial chloride channel regulated by phosphorylation of serines in the regulatory domain of the channel (most prominently by protein kinase A; Cheng et al., 1991; Tabcharani et al., 1991), and by binding (Venglarik et al., 1994) or hydrolysis (Baukrowitz et al., 1994; Gunderson and Kopito, 1994) of ATP. The most characteristic gating of CFTR in both endogenously expressing epithelial cells and in recombinantly expressing systems was the presence of long (several hundred milliseconds) open bursts broken by fast (millisecond) closures (Gray et al., 1989; Haws et al., 1992; Fischer and Machen, 1994a).

Because CFTR occurs in high number, plasma membrane patches generally contain multiple channels, and gating characteristics are therefore best described in noise analytical terms. In the frequency domain, CFTR's gating translates into a low-frequency Lorentzian of ~1 Hz and a high-frequency Lorentzian of ~100 Hz (Fischer and Machen, 1994a). The low-frequency Lorentzian was shown to be dependent on the ATP and ADP concentrations at the intracellular face of the channel (Venglarik et al., 1994; Schultz et al., 1995) and appears therefore related to slow, ATP-dependent opening and closing of the channel. The high-frequency Lorentzian, i.e., the fast gate of the channel, is poorly understood. Early on, Gray et al. (1989) showed that the high-frequency gating was strongly voltage-dependent, such that fast gating was extremely reduced at depolarizing potentials, and it has been suggested that an intracellular anionic factor serves as a fast, reversible blocker (Overholt et al., 1993; Fischer and Machen, 1994b). Under physiological conditions the high-frequency Lorentzian describes a major gating event of the channel.

The cellular proto-oncogene $p60^{c\text{-}src}$ (src) is a cytosolic nonreceptor tyrosine kinase. Tyrosine phosphorylation mediates numerous cellular processes including signal transduction and propagation of mitogenic and transforming signals (Cantley et al., 1991; Fischer et al., 1991). Several plasma membrane ion channels appear to be regulated by tyrosine phosphorylation, for example, the acetyl choline receptor channel (Huganir et al., 1984) and a voltage-gated cation channel in neurons (Wilson and Kaczmarek, 1993); the epithelial Na channel in kidney cells (Matsumoto et al., 1993); and the Ca entry channel in chloride secretory epithelial cells (Bischof et al., 1994); and in fibroblasts (Lee et al., 1993).

In this paper we show that src has major effects on CFTR's gating both in the airway cell line Calu-3 expressing CFTR endogenously, and in CFTR-transfected 3T3 fibroblasts. Because channel gating after src treatment restored the general characteristics of CFTR's gating in the cell-attached mode, we suggest that tyrosine phosphorylation is a physiological determinant of CFTR's behavior.

Received for publication 15 December 1995 and in final form 27 August 1996.

Address reprint requests to Dr. Horst Fischer, University of Pittsburgh, Department of Cell Biology and Physiology, 818E Scaife Hall, 3550 Terrace Street, Pittsburgh, PA 15261. Tel.: 412-383-8858; Fax: 412-648-8330; E-mail: fisch+@pitt.edu.

0006-3495/96/12/3073/10 $2.00

METHODS

Cells

Mouse fibroblast National Institutes of Health 3T3 cells stably transfected with the wild-type CFTR, and the airway epithelial cell line Calu-3 (Haws et al., 1994), were cultured with standard cell culture techniques. 3T3 cells were grown in antibiotic-free H-21 Dulbecco's minimal essential medium (DMEM) supplemented with 10% newborn calf serum; Calu-3 cells were grown in DMEM supplemented with 10% fetal calf serum and 4 mM glutamine (all from Univ. of California at San Francisco Cell Culture Facility). Cells were seeded in low density on glass coverslips and were used after 1 to 2 days. The gating characteristics were indistinguishable between the recombinant CFTR in 3T3's and the endogenous CFTR in Calu-3's.

Patch clamp recordings

All measurements and manipulations were performed on the stage of a microscope in an open, perfusable chamber (~0.5 ml) at 37°C as described before (Fischer and Machen, 1994a). Briefly, patch pipettes were pulled from thick-walled borosilicate glass (Corning 7052, World Precision Instruments, FL) to yield, after filling and fire-polishing, resistances of ~10 MW. After seal formation, currents were continuously recorded to a computer hard disk. All recordings in this report contained multiple channels. In the cell-attached mode the applied potential is reported as the negative pipette potential ($-V_p$), and in the excised mode as the membrane potential (V_m). Average currents (I) of multichannel recordings are reported after subtraction of baseline currents. If not mentioned specifically, currents were sampled at 5 kHz and filtered at 500 Hz.

The same current signal was high-pass filtered (0.03 Hz to remove the DC current component), low-pass filtered and further amplified 10×. The resulting AC-noise signal was fed into a second computer which performed on-line Fast Fourier transforms. The fundamental frequency (Δf) was variable. The upper bandwidth limit was given by $1600\times\Delta f$, e.g., for our standard setting of $\Delta f = 0.25$ Hz the signal was low-pass filtered at 400 Hz. In order to increase the analyzed frequency window, in some cases spectra were generated from overlapping windows and then merged. At least 12 consecutive time intervals (each consisting of 4096 samples) were analyzed, resulting in an average spectrum. Spectral densities (S) were plotted in log-log plots and fitted with the sum of two Lorentzians of the form

$$S = S_{0l}/[1 + (f/f_{cl})] + S_{0h}/[1 + (f/f_{ch})^2] \quad (1)$$

resulting in fit-estimates of the corner frequencies (f_{cl}, f_{ch}) and the amplitudes (S_{0l}, S_{0h}) of the low- (l) and the high- (h) frequency Lorentzians. In cases where the spectral densities at increasing frequencies approached background noise levels, high-frequency points were excluded for fits as noted.

The noise (σ^2) generated by each Lorentzian is given by its integral or

$$\sigma_x^2 = f_{cx} * S_{0x} * \pi/2 \quad (2)$$

with x = l or x = h for the low- or the high-frequency Lorentzian. Then the relative contribution of the high-frequency Lorentzian to total noise (in %) is given by

$$\sigma_{hr}^2 = 100 * \sigma_h^2/(\sigma_l^2 + \sigma_h^2), \quad (3)$$

which was used to quantify the activity of the fast gate. All recordings in this report contained multiple CFTRs per patch, but some current records in the figures were selected from those with relatively few (<5) open levels per patch in order to display gating more clearly.

Solutions and chemicals

The composition of the standard bath solution was (in mM): 141 NaCl, 4 KCl, 1 KH_2PO_4, 1 $MgCl_2$, 1.7 $CaCl_2$, 10 Hepes, 25 glucose, pH = 7.3. Pipette filling solution was (in mM): 147 *N*-methyl-D-glucamine chloride (NMDG-Cl), 1.7 $CaCl_2$, 10 Hepes, 25 glucose, pH = 7.3. Bath solution for excised patches was (in μM): 147 NMDG-Cl, 1.7 $MgCl_2$, 0.1 EGTA, 1 MgATP, 25 glucose, pH = 7.3. Forskolin (Calbiochem, La Jolla, CA), the adenylyl cyclase activator, was made as a 100-mM stock in dimethyl sulfoxide and used at 1–10 μM. The catalytic subunit of protein kinase A (Promega, Madison, WI) was used at a final activity of 33–100 units/ml, and the recombinant $p60^{c\text{-}src}$ (Upstate Biotechnology Inc, Lake Placid, NY) was used at 0.5–10 units per bath, i.e., ~1-20 units/ml. Neither PKA nor src showed concentration-dependent effects in the used activity range. For stability the src preparation contained 50% glycerol, which was diluted during use to 0.016–0.33%. In control experiments up to 1.84% (=200 mM) glycerol added to excised patches had no effects on CFTR-mediated currents or its gating characteristics (see Results, Fig. 7). In another set of control experiments for glycerol contents, the src preparation was centrifuged for 3 h at 6000 × g through a 5000 mol wt cutoff filter and resuspended in bath solution. However, this treatment greatly reduced src activity; therefore, all experiments shown in this report were performed with the original glycerol-containing src preparation. Lambda protein phosphatase (λPP, New England Biolabs, Beverly, MA), a viral serine/threonine/tyrosine phosphatase, was used at 200 units/ml in the presence of 0.17 mM $MnCl_2$, 80 mg/ml bovine serum albumin, and 0.125% glycerol. There were no effects of these additives on CFTR gating. Na_3VO_4 was made as a 100-mM stock in 50 mM tris[hydroxymethyl]aminomethane at pH = 10.0, stored in the dark at 4°C and used at 1 mM in NMDG-Cl solution.

Statistics

All data are given as originals or as means ± SEM. Statistics were calculated with the statistics package BMDP New System (BMDP Statistical Software, Inc., Los Angeles, CA) employing one-way and two-way analyses of variance (ANOVA). Probabilities (p) of contrasts between groups were calculated with Student's t-tests, or Mann-Whitney tests for non-normal distributions. A $p < 0.05$ was considered statistically significant. The fitting procedure for current noise spectra was described earlier in detail (Fischer and Machen, 1994a).

RESULTS AND DISCUSSION

Fig. 1 shows a recording from a cell-attached patch clamp recording on a forskolin-stimulated Calu-3 cell. All recordings in this report contained multiple channels per patch. Identical to what we reported earlier for the recombinant CFTR expressed in 3T3 cells (Fischer and Machen, 1994a), the endogenous CFTR of Calu-3 cells showed marked voltage-dependence of its fast gate as shown previously (Haws et al., 1994). Fig. 1 *A* shows current traces at $-V_p = +88$ mV (*top*) and at $-V_p = -88$ mV (*bottom*). At positive potentials CFTR's gating was characterized by long-lasting openings and closings, and only few fast events were discernible. At negative potentials, where chloride moves in the physiological direction (i.e., out of the cell), long-lasting openings were broken by numerous fast closings resulting in CFTR's typical burstlike activity.

The voltage-dependent gating of CFTR was quantified in the current noise spectra shown in Fig. 1 *B*. Spectra contained two Lorentzian noise components. The low-frequency Lorentzian's corner frequency was, on average, $f_{cl} = 1.69 \pm 0.125$ Hz ($n = 50$) and showed no dependence on the applied voltage (Fig. 2). In contrast, the high-frequency Lorentzian was strongly dependent on the applied voltage in the cell-attached mode. It was clearly present at

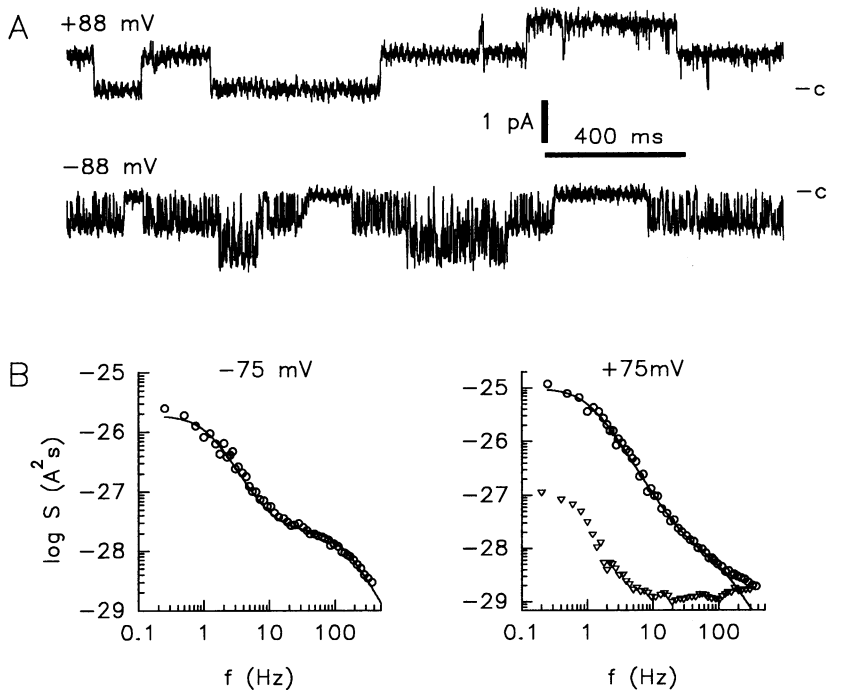

FIGURE 1 Cell-attached recording from a Calu-3 cell stimulated with 1 μM forskolin. (*A*) Current traces at $-V_p$ = 88 mV (*top*) and −88 mV (*bottom*) show fast and slow gating of CFTR in the cell-attached mode and the fast gate's dependence on negative holding potential. c denotes all-closed level. (*B*) Spectra of CFTR-generated current noise at $-V_p$ = −75 mV (*left*) and $-V_p$ = +75 mV (*right*). The low-frequency Lorentzian was prominent at both voltages, while the high-frequency Lorentzian was considerably diminished at positive $-V_p$. Fit results for the spectra are, at $-V_p$ = −75 mV (*left panel*, f_{cl}, f_{ch}, S_{0l}, S_{0h}): 1.14 Hz, 128 Hz, 1.87E-26 A^2s, 2.21E-28 A^2s; and at $-V_p$ = 75 mV (*right panel*, f_{cl}, f_{ch}, S_{0l}, S_{0h}): 1.01 Hz, 91.6 Hz, 9.84E-26 A^2s, 7.91E-29 A^2s. For the spectrum at +75 mV points >100 Hz were excluded from the fit because noise intensities approached background noise levels. Triangles show a background noise spectrum of a recording containing no active channels.

negative potentials (Fig. 1 *B*, *left panel*), while at positive potentials both its corner frequency (f_{ch}) and its power were significantly reduced, such that it contributed very little to the total current fluctuations (Fig. 1 *B*, *right panel*). In several cases the high-frequency Lorentzian could not be fitted reliably because it approached background noise levels (*right panel*, ▽). Fig. 2, *A* and *B* (left pair of bars, respectively) show averages-of-fit results of the low- and high-frequency Lorentzians at positive and negative potentials in the cell-attached mode.

In addition to the effects of voltage, excision of a membrane patch also had major effects on CFTR's fast gate (Fig. 3). The recording in Fig. 3 *A* shows a patch excised from a forskolin-stimulated 3T3 cell. In the cell-attached mode CFTR displayed its typical bursting at negative potentials (Fig. 3 *A*). Immediately after patch excision (Fig. 3 *A*, *arrow*) this fast gating was virtually lost when compared to that exhibited before excision. Fig. 3 *B* quantifies the steady-state kinetics before (*left panel*) and after excision (*right panel*). The cell-attached spectrum shows a prominent high-frequency Lorentzian that was greatly reduced after excision of the patch (*right panel*). The relative contribution of the high-frequency Lorentzian to total gating noise in the cell-attached mode was σ^2_{hr} = 57.5%, and was reduced to σ^2_{hr} = 14.9% after excision (for averages see Fig. 2 *C*). The amplitude of the high-frequency Lorentzian was extremely diminished at all potentials in the excised mode, while f_{ch} was unchanged and still retained its voltage dependence (Fig. 2 *B*). This suggested that the underlying mechanism of the fast gate remained functional but operated on a much lower level.

Most of the patch excisions in this report showed immediate (<1 s) reduction of fast gating as in Fig. 3, but in 4 of 39 cases fast gating remained relatively unchanged for up to ~30 s following excision. Fig. 4 shows a patch excision from a forskolin-stimulated Calu-3 cell where the fast gate stayed active for ~2 s after excision. This behavior is consistent with the notion that a diffusible factor is lost after excision, and this effect is dependent on diffusion barriers, which are variable from patch to patch. Note that excision of a patch increased the single-channel amplitude of CFTR compared to cell-attached (Figs. 3 *A* and 4). This is explained in part by the increased chloride concentration at the intracellular side of the channel, but may also reflect the reduction of rapid gating events after excision, which led to diminished single channel currents due to frequency limitations in the cell-attached mode. Consistent with this, immediately after excision, in Fig. 4 the single-channel amplitude increased slightly (i = 0.72 pA) over levels before excision (i = 0.68 pA), and after the inactivation of the fast gate i = 0.82 pA.

Excision into solution containing 1 mM ATP shifted the low-frequency Lorentzian significantly to the right (Figs. 2 *A* and 3 *B*). Previously, the low-frequency Lorentzian was shown to be dependent on the concentrations of ATP and ADP at the intracellular side of the channel. Increasing [ATP] increased f_{cl} and increasing [ADP] decreased f_{cl} (Venglarik et al., 1994; Schultz et al., 1995). Thus, f_{cl} is likely to be affected by the changes in [ATP] and [ADP] when a cell-attached patch was excised into 1 mM ATP-containing solution.

In summary, the high-frequency Lorentzian was dependent on the recording conditions, being increased in intensity by negative potentials (compared to positive potentials) and reduced by patch excision (compared to cell-attached). The strong voltage-dependence points to a factor in the

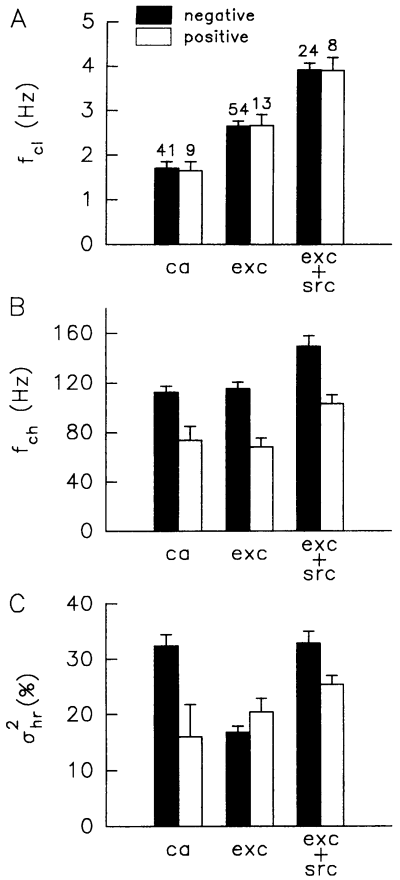

FIGURE 2 Average-fit results of Lorentzian parameters. Conditions were: ca, cell-attached; exc, excised in presence of 1 mM MgATP, PKA-phosphorylated, or after forskolin-stimulation of intact cells; exc+src, excised in presence of 1 mM MgATP and src tyrosine kinase; filled bars, negative potentials (pooled over a range from −60 to −90 mV); open bars, positive potentials (pooled over a range from 60 to 90 mV). (*A*) f_{cl} was significantly dependent on the condition (p = 2E-15) but not on potential (p = 0.94, two-way ANOVA). Cell-attached f_{cl} was significantly lower (1.69 ± 0.12 Hz, n = 50, all potentials pooled, p = 0.0) and exc+src significantly higher (3.91 ± 0.14 Hz, n = 32, p = 2E-7) than exc f_{cl} (2.65 ± 0.11 Hz, n = 67). Numbers in *A* give number of fitted spectra for each bar. (*B*) f_{ch} was significantly dependent on both condition (p = 3E-4) and potential (p = 1E-8, two-way ANOVA). For negative potentials, f_{ch} during exc+src treatment was significantly higher than during cell-attached (p = 1E-4) and excised (p = 2E-4) recordings, which were not different from one another. For positive potentials, f_{ch} was increased after src treatment over cell-attached (p = 0.03) and excised (p = 0.008), which were not different. (*C*) σ^2_{hr}, the relative contribution of the high-frequency noise to total noise [eq. (3)], showed significant voltage dependence in the cell-attached mode (p = 7E-4) and during src treatment (p = 0.046), but not in the excised mode (p = 0.21). At negative potentials σ^2_{hr} values after excision were significantly lower than cell-attached values (p = 9E-11), and src treatment restored σ^2_{hr} to values similar to those observed under cell-attached conditions (p = 0.55). At positive potentials σ^2_{hr} was significantly increased during src treatment (p = 0.021) compared to cell-attached values. All pairwise comparisons for σ^2_{hr} were performed using nonparametric Mann-Whitney test statistics owing to the non-normal, left-skewed distributions of σ^2_{hr}.

electrical field of the membrane. A simple idea is an anionic cellular diffusible factor that rapidly blocks the channel when pulled into the pore by the membrane potential, as suggested earlier (Overholt et al., 1993; Fischer and Machen, 1994b). In support of this idea, the anionic compounds diphenylcarboxylate and flufenamate induced similar short-lived and highly voltage-dependent blocking events in excised CFTR (McCarty et al., 1993). In intact cells such blocking events could be assumed by anionic, impermeant amino acids (Overholt et al., 1993).

Another explanation for the characteristics of the high-frequency Lorentzian could be a labile phosphorylation that gets cleaved after patch excision. Phosphotyrosines can be expected to be quickly dephosphorylated in isolated membrane patches owing to the ubiquitous presence of membrane-associated tyrosine phosphatases (Fischer et al., 1991). A phosphotyrosine within the field of the membrane could have voltage-dependent effects on the permeation pathway. Therefore, we tested for effects of tyrosine phosphorylation of CFTR by applying the tyrosine kinase src to excised patches.

Addition of src to unstimulated patches had no effects, i.e., src did not stimulate CFTR in silent patches (n = 2, not shown). However, addition of src to excised patches containing active CFTR significantly affected CFTR-mediated currents and their gating behavior. Fig. 5*A* shows a condensed trace of total current across an excised patch containing multiple channels. Addition of src (10 units) stimulated current (in this run from −3.2 pA to −5.9 pA). On average, mean current increased to 154 ± 29% of levels before src addition (n = 13, including 4 nonresponders, significantly different from 100%, nonparametric sign test, $p < 0.004$). Fig. 5 *B* shows high-resolution traces from the condensed trace in 5 *A*. The top trace shows clearly identifiable channel events in this multichannel patch. Addition of src changed CFTR's gating behavior considerably (Fig. 5 *B, lower trace*). A significant increase in fast gating was readily distinguishable from the current trace. Current fluctuations were quantified in the corresponding spectra shown in Fig. 5 *C*. The spectrum recorded after excision (*open circles*) showed the typical two Lorentzians with a low-intensity high-frequency Lorentzian (f_{ch} = 93 Hz, σ^2_{hr} = 18.7%). Src treatment (*filled circles*) significantly increased the high-frequency Lorentzian noise component. In this experiment f_{ch} increased to 120 Hz, and σ^2_{hr} increased to 40.5%. Average values of fit results after src addition are given in Fig. 2. Src restored the typical voltage dependence of both the amplitude of the high-frequency Lorentzian and f_{ch}. Fig. 6*A* shows two spectra recorded from an excised patch in the presence of src at V_m = −60 mV (*filled circles*), and V_m = 60 mV (*open circles*). The high-frequency Lorentzian showed voltage dependence with f_{ch} decreasing from 131 Hz to 114 Hz, and σ^2_{hr} decreasing from 33% to 25% after stepping from V_m = −60 mV to V_m = +60 mV. See Fig. 2, *B* and *C* for averages of voltage-dependent changes.

Therefore, addition of src to excised patches recovered the typical gating characteristics of CFTR when recorded from intact cells, i.e., in the cell-attached mode. Src recovered the high-frequency Lorentzian and also its voltage

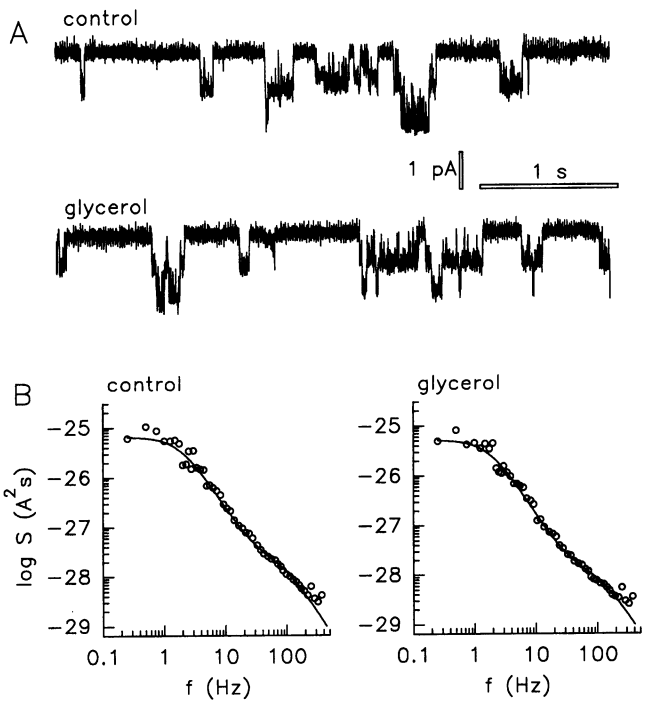

FIGURE 7 Effects of glycerol on CFTR. Patch was excised from a forskolin-stimulated 3T3 cell. (*A*) CFTR activity in 1 mM ATP (control) and after addition of 200 mM glycerol in bath solution (glycerol). (*B*) Spectra showing control activity, f_{cl} = 1.88 Hz, f_{ch} = 82.3 Hz, S_{0l} = 6.49E-26 A^2s, S_{0h} = 2.38E-28 A^2s, and in the presence of 200 mM glycerol, f_{cl} = 1.75 Hz, f_{ch} = 104 Hz, S_{0l} = 5.3E-26 A^2s, S_{0h} = 1.2E-28 A^2s. Fits of the high-frequency Lorentzians were uncertain because of the low expression of high-frequency gating in both cases. Spectra were recorded from 60 s control and glycerol treatment, respectively, of which 4 s are shown in *A* and *B*, respectively.

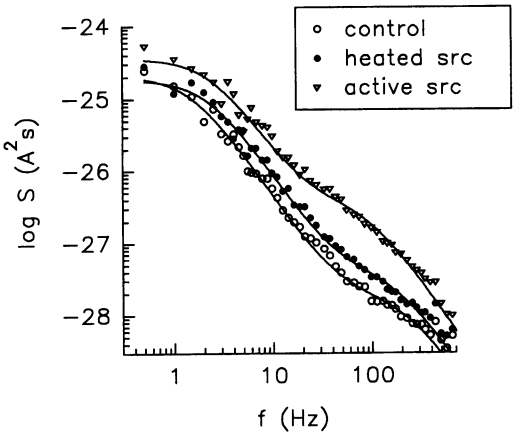

FIGURE 8 Control experiment for possible contaminants in the preparation. The src preparation was heat-inactivated (45°C for 15 min) and then tested on CFTR. PKA activation elicited normal gating behavior for excised patches (○; f_{cl} = 1.46 Hz, f_{ch} = 206 Hz, S_{0l} = 2.1E-25 A^2s, S_{0h} = 1.7E-28 A^2s). Addition of heat-inactivated src (●) corresponding to 6 units of the intact preparation affected spectrum only minimally (possibly due to residual src activity; f_{cl} = 2.16 Hz, f_{ch} = 173 Hz, S_{0l} = 1.85E-25 A^2s, S_{0h} = 3.7E-28 A^2s). Addition of 3 units intact src (▽) resulted in typical change of CFTR spectrum (f_{cl} = 2.72 Hz, f_{ch} = 97.6 Hz, S_{0l} = 2.5E-25 A^2s, S_{0h} = 3.3E-27 A^2s. Excised from a 3T3 cell, 1 mM ATP, V_m = −75 mV.

9 *B*) showed the typical src-induced changes (*filled circles*), which were reduced by λPP treatment (*triangles*). Note that all additions in this experiment were in standing solution, and the final current corresponded to an equilibrium of all enzyme activities. λPP inactivated src effects on both current and gating, indicating that src effects depended on tyrosine phosphorylation.

Patch excision elicited a loss of CFTR's high-frequency gating, and addition of src in the presence of ATP restored this rapid gating. We hypothesized that the explanation for this behavior was that patch excision led to loss of cellular tyrosine kinases, while a membrane-associated tyrosine phosphatase de-phosphorylated tyrosine(s). We tested this possibility in two sets of experiments. First we tested effects of sequential addition and removal of src. Results from one of these experiments are shown in Fig. 10. During src treatment (*open circles*), the typical high-frequency Lorentzian was present (σ^2_{hr} = 27.8%). When src was washed out (*filled circles*), the high-frequency Lorentzian was diminished (σ^2_{hr} = 18.1%). The high-frequency Lorentzian was restored again by a second addition of src (*triangles*, σ^2_{hr} = 35.2%) indicating that the actual presence of src was necessary to maintain high-frequency gating, and likely to maintain the tyrosine phosphorylation level of CFTR.

In a second set of experiments we tested for the presence of patch-associated tyrosine phosphatases by excising cell-attached patches into solution containing sodium orthovanadate (1 mM, n = 4), a tyrosine phosphatase inhibitor (Brautigan and Shriner, 1988). Fig. 11 shows recordings of the CFTR in the cell-attached mode (Fig. 11 *A*) and after excision (Fig. 11 *B*) into vanadate. After excision the high-frequency gating and Lorentzian stayed active (Fig. 11 *B*), consistent with the block of a tyrosine phosphatase by vanadate. High-frequency gating was likely not induced by a direct vanadate-channel interaction, because when vanadate was applied after excision, fast gating was not rescued (1 mM, n = 9, not shown). Fig. 11 *B* (*bottom panel*) also shows the typical "open locking" of CFTR (Baukrowitz et al. 1994), which is related to vanadate's block of CFTR's ATPase activity. This side-effect of vanadate led to nonstationary conditions within the analyzed frequency window so that vanadate's effects on high-frequency gating were difficult to quantify by our approach of relating high-frequency noise to total noise. The righthand panels in Fig. 11, *A* and *B* show spectra of cell-attached CFTR and after excision. The cell-attached spectrum shows the typical characteristics of slow and fast gating. After excision into vanadate (Fig. 11 *B*) the high-frequency Lorentzian remained intact while the low-frequency range was not fitable, likely due to the distortion of slow kinetics by long-lasting openings. These results suggested that a patch-associated tyrosine phosphatase was responsible for the reduction of fast gating after excision, which remained intact when the tyrosine phosphatase was blocked with vanadate.

The effect of the tyrosine kinase src and its inactivation by λPP, and the effects of the tyrosine phosphatase

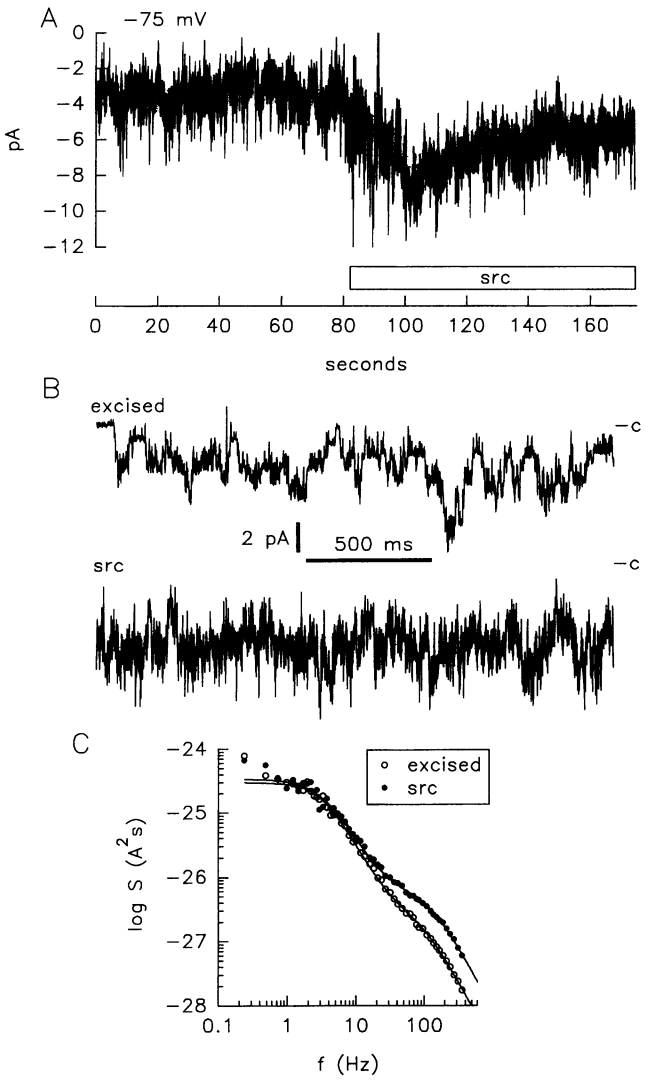

FIGURE 5 Effects of src on gating of CFTR. Patch was excised from a forskolin-stimulated 3T3 fibroblast expressing recombinant CFTR. V_m = −75 mV. 1 mM MgATP was present in bath throughout. (*A*) Condensed current recording. Addition of src stimulated average current. Sampled at 20 Hz. (*B*) *Top trace:* Detail from Fig. 4 at 67 s, CFTR activity after excision, slow gating is apparent. *Bottom trace:* Gating in presence of src showed notably more high-frequency gating. c denotes the all-closed level. (*C*) Corresponding current noise spectra. Both spectra (excised, ○; src, ●) expressed two Lorentzians. Src significantly increased the high-frequency component. Fitted parameters were: excised (○, f_{cl}, f_{ch}, S_{0l}, S_{0h}) 3.06 Hz, 92.9 Hz, 3.35E-25 A^2s, 2.54E-27 A^2s; and src (●, f_{cl}, f_{ch}, S_{0l}, S_{0h}) 3.6 Hz, 120.3 Hz, 2.93E-25 A^2s, 5.98E-27 A^2s.

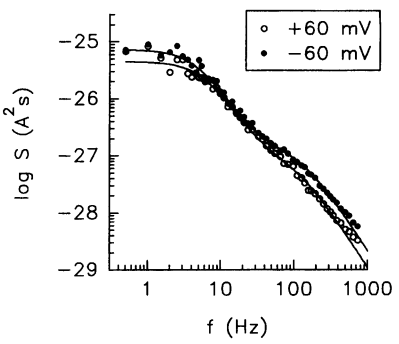

FIGURE 6 Voltage-dependence of CFTR after src treatment. Current noise spectra recorded from an excised patch in presence of src after PKA phosphorylation. Fitted values were: (●; V_m = −60 mV, f_{cl}, f_{ch}, S_{0l}, S_{0h}): 4.46 Hz, 130.7 Hz, 7.2E-26 A^2s, 1.21E-27 A^2s, and (○; V_m = 60 mV, f_{cl}, f_{ch}, S_{0l}, S_{0h}): 5.71 Hz, 114.3 Hz, 4.41E-26 A^2s, 7.43E-28 A^2s.

Fast gating of CFTR consists mainly of rapid closures (Fig. 1), corresponding to the short-lived closed$_2$ state in the scheme above. The high-frequency Lorentzian is therefore given by the righthand open–closed$_2$ transition with the closing rate γ and opening rate δ. Because the high-frequency Lorentzian showed very low powers in excised patches, the close$_2$ state appeared to be an infrequent event and, therefore, the closing rate γ was low. Under these conditions $\gamma \ll \delta$, or $2\pi f_{ch}$ approximates δ. Addition of src increased f_{ch} and S_{0h}, indicating an increase in the closing rate γ. Since src had effects on both the low- and the high-frequency Lorentzians, which reflect functionally independent events, and in the gating model above at least two rate constants were affected (α and γ), our data support the notion that src had effects on both ATP-dependent openings and voltage-dependent sites within the pore of CFTR.

We also tested whether the observed src effects were related to src's kinase activity or to other factors or contaminants present in the src preparation. The src preparation contained high amounts (50%) of glycerol to increase the stability of src in solution. Under our recording conditions the glycerol concentration was diluted during use to 0.016–0.33% In control experiments for effects of glycerol, up to 1.84% (= 200 mM) had no effects on channel gating. Fig. 7 shows a recording and the corresponding spectra from an excised patch before and after 200 mM glycerol. No effects of glycerol were apparent in this and four other controls using concentrations of 100 mM or 200 mM glycerol.

Then we tested a heat-inactivated src preparation in order to distinguish effects related to src's phosphorylation activity from possible effects of other contaminants in the preparation. The original preparation was inactivated for 15 min at 45°C in a water bath. Fig. 8 shows current noise spectra of CFTR generated current fluctuations after PKA stimulation (*open circles*), after heat-inactivated src treatment (*filled circles*), and after treatment with the intact src preparation (*open triangles*). Heat-inactivated src affected the spectrum only slightly, while active src elicited the typical changes in the spectrum; i.e., increased amount of fast gating and increased f_{cl}, suggesting that src effects were related to the phosphorylation activity of src.

If src effects relied on a phosphorylation it can be expected that a phosphatase would reverse its effects. We used the nonspecific serine/threonine/tyrosine phosphatase lambda phosphatase (λPP). Fig. 9 shows a PKA activation of CFTR currents, followed by further src activation, and finally inactivation by λPP. The first addition of src (3 units) had only small effects, but the second src addition (3 units) stimulated current significantly. Current noise spectra (Fig.

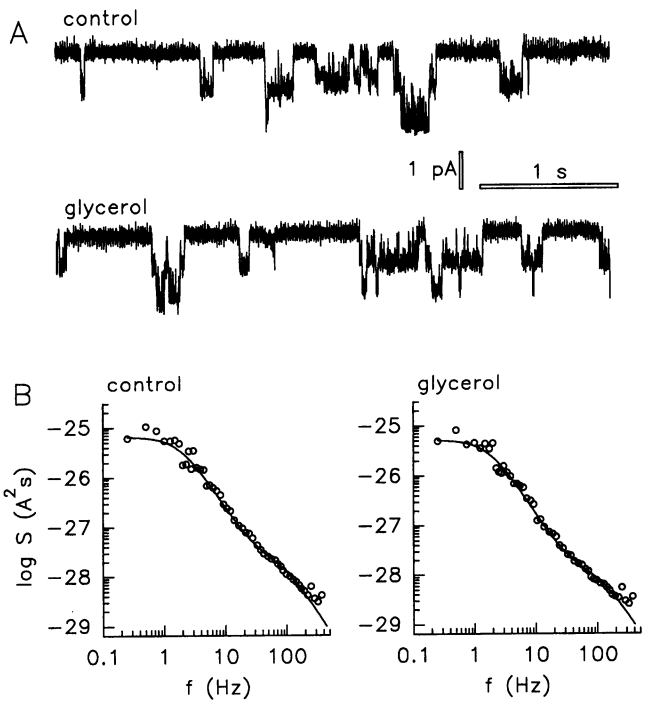

FIGURE 7 Effects of glycerol on CFTR. Patch was excised from a forskolin-stimulated 3T3 cell. (*A*) CFTR activity in 1 mM ATP (control) and after addition of 200 mM glycerol in bath solution (glycerol). (*B*) Spectra showing control activity, f_{cl} = 1.88 Hz, f_{ch} = 82.3 Hz, S_{0l} = 6.49E-26 A^2s, S_{0h} = 2.38E-28 A^2s, and in the presence of 200 mM glycerol, f_{cl} = 1.75 Hz, f_{ch} = 104 Hz, S_{0l} = 5.3E-26 A^2s, S_{0h} = 1.2E-28 A^2s. Fits of the high-frequency Lorentzians were uncertain because of the low expression of high-frequency gating in both cases. Spectra were recorded from 60 s control and glycerol treatment, respectively, of which 4 s are shown in *A* and *B*, respectively.

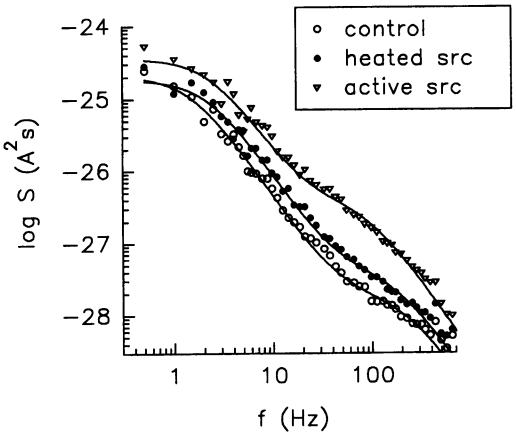

FIGURE 8 Control experiment for possible contaminants in the preparation. The src preparation was heat-inactivated (45°C for 15 min) and then tested on CFTR. PKA activation elicited normal gating behavior for excised patches (○; f_{cl} = 1.46 Hz, f_{ch} = 206 Hz, S_{0l} = 2.1E-25 A^2s, S_{0h} = 1.7E-28 A^2s). Addition of heat-inactivated src (●) corresponding to 6 units of the intact preparation affected spectrum only minimally (possibly due to residual src activity; f_{cl} = 2.16 Hz, f_{ch} = 173 Hz, S_{0l} = 1.85E-25 A^2s, S_{0h} = 3.7E-28 A^2s). Addition of 3 units intact src (▽) resulted in typical change of CFTR spectrum (f_{cl} = 2.72 Hz, f_{ch} = 97.6 Hz, S_{0l} = 2.5E-25 A^2s, S_{0h} = 3.3E-27 A^2s. Excised from a 3T3 cell, 1 mM ATP, V_m = −75 mV.

9 *B*) showed the typical src-induced changes (*filled circles*), which were reduced by λPP treatment (*triangles*). Note that all additions in this experiment were in standing solution, and the final current corresponded to an equilibrium of all enzyme activities. λPP inactivated src effects on both current and gating, indicating that src effects depended on tyrosine phosphorylation.

Patch excision elicited a loss of CFTR's high-frequency gating, and addition of src in the presence of ATP restored this rapid gating. We hypothesized that the explanation for this behavior was that patch excision led to loss of cellular tyrosine kinases, while a membrane-associated tyrosine phosphatase de-phosphorylated tyrosine(s). We tested this possibility in two sets of experiments. First we tested effects of sequential addition and removal of src. Results from one of these experiments are shown in Fig. 10. During src treatment (*open circles*), the typical high-frequency Lorentzian was present (σ^2_{hr} = 27.8%). When src was washed out (*filled circles*), the high-frequency Lorentzian was diminished (σ^2_{hr} = 18.1%). The high-frequency Lorentzian was restored again by a second addition of src (*triangles*, σ^2_{hr} = 35.2%) indicating that the actual presence of src was necessary to maintain high-frequency gating, and likely to maintain the tyrosine phosphorylation level of CFTR.

In a second set of experiments we tested for the presence of patch-associated tyrosine phosphatases by excising cell-attached patches into solution containing sodium orthovanadate (1 mM, n = 4), a tyrosine phosphatase inhibitor (Brautigan and Shriner, 1988). Fig. 11 shows recordings of the CFTR in the cell-attached mode (Fig. 11 *A*) and after excision (Fig. 11 *B*) into vanadate. After excision the high-frequency gating and Lorentzian stayed active (Fig. 11 *B*), consistent with the block of a tyrosine phosphatase by vanadate. High-frequency gating was likely not induced by a direct vanadate-channel interaction, because when vanadate was applied after excision, fast gating was not rescued (1 mM, n = 9, not shown). Fig. 11 *B* (*bottom panel*) also shows the typical "open locking" of CFTR (Baukrowitz et al. 1994), which is related to vanadate's block of CFTR's ATPase activity. This side-effect of vanadate led to nonstationary conditions within the analyzed frequency window so that vanadate's effects on high-frequency gating were difficult to quantify by our approach of relating high-frequency noise to total noise. The righthand panels in Fig. 11, *A* and *B* show spectra of cell-attached CFTR and after excision. The cell-attached spectrum shows the typical characteristics of slow and fast gating. After excision into vanadate (Fig. 11 *B*) the high-frequency Lorentzian remained intact while the low-frequency range was not fitable, likely due to the distortion of slow kinetics by long-lasting openings. These results suggested that a patch-associated tyrosine phosphatase was responsible for the reduction of fast gating after excision, which remained intact when the tyrosine phosphatase was blocked with vanadate.

The effect of the tyrosine kinase src and its inactivation by λPP, and the effects of the tyrosine phosphatase

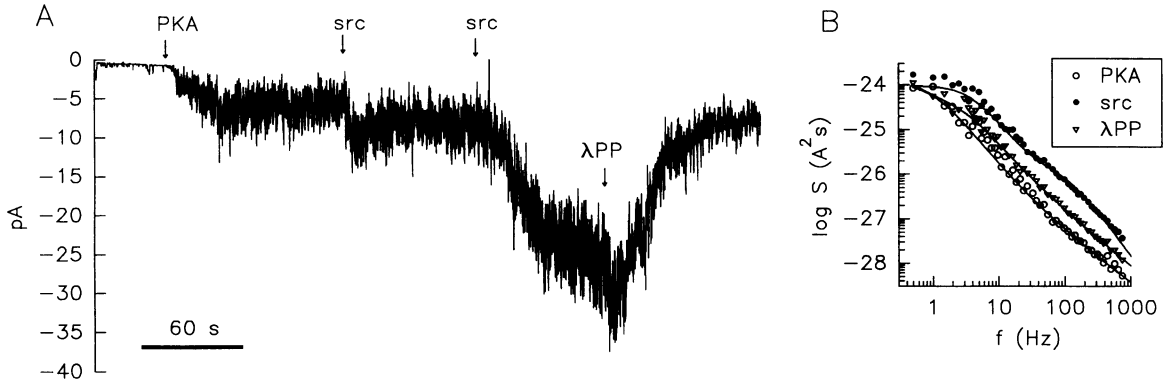

FIGURE 9 Inactivation of src effects by λPP. (*A*) Condensed current recording. Patch was excised from a 3T3 cell and stimulated with PKA (25 units). The first src addition (3 units) stimulated current moderately, second src addition (3 units) led to a sustained increase of current. Addition of λPP (100 units) inactivated current. All enzyme additions were in standing solution so that the final current reflects an equilibrium of all enzyme activities. $V_m = -70$ mV, sampled at 20 Hz. (*B*) Current noise spectra were recorded after PKA stimulation, after the second src addition, and after λPP inactivation of current. Fitted parameters were for PKA (○) $f_{cl} = 1.2$ Hz, $S_{0l} = 8.1E\text{-}25$ A^2s; src (●) $f_{cl} = 3.97$ Hz, $f_{ch} = 104$ Hz, $S_{0l} = 9.4E\text{-}25$ A^2s, $S_{0h} = 1.3E\text{-}26$ A^2s; λPP (▽) $f_{cl} = 3.14$ Hz, $S_{0l} = 3.1E\text{-}25$ A^2s. Spectra after PKA and after λPP did not permit to fit a second Lorentzian because high-frequency gating was little expressed. Instead, spectra were fitted together with a linear background to better approximate data.

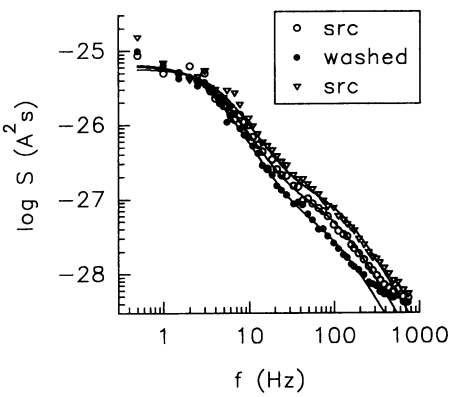

FIGURE 10 Src-induced gating behavior is transient in excised patches. Current noise spectra recorded from an excised CFTR-containing patch from a 3T3 cell after PKA-phosphorylation in presence of 1 mM ATP. ○, in presence of src the high-frequency Lorentzian was prominent; ●, after wash-out of src the high-frequency Lorentzian was greatly reduced; ▽, after renewed src addition the high-frequency Lorentzian reappeared. Excised, $V_m = 60$ mV, 1 mM MgATP. Fitted values were: ○, f_{cl}, f_{ch}, S_{0l}, S_{0h}, 3.46 Hz, 102 Hz, 6.17E-26 A^2s, 8.1E-28 A^2s; ●, 2.94 Hz, 98.9 Hz, 6.54E-26 A^2s, 4.3E-28 A^2s; ▽, 4.37 Hz, 120.9 Hz, 5.6E-26 A^2s, 1.1E-27 A^2s. All fits were performed by omitting high-frequency points beyond 380 Hz, 250 Hz, and 530 Hz, for ○, ●, and ▽, respectively.

blocker vanadate, support the notion that a phosphotyrosine is an important regulator of CFTR's gating. Its voltage dependence points to a phosphotyrosine that lies within the field of the membrane that is accessible to src. CFTR's amino acid sequence contains multiple tyrosines on its cytosolic side present in all functional domains of the protein, including the transmembrane domains, the nucleotide binding domains (NBDs), and the regulatory domain. Since the three-dimensional configuration of the CFTR is unknown, it is unclear which tyrosines might be accessible for src kinase, and we can only speculate about possible sites. One intriguing site could be Tyr-84, because it is located in the first transmembrane segment, which was previously shown to be part of the pore (Anderson et al., 1991; Akabas et al., 1994) and therefore would sense the membrane potential. In addition, its setting in the amino acid sequence Arg^{80}-Phe^{81}-Met^{82}-Phe^{83}-Tyr^{84}-Gly^{85}-Ile^{86}-Phe^{87}-Leu^{88} predicts Tyr-84 as a possible phosphorylation site for src (Songyang et al., 1995). Six tyrosines are also present in the first NBD, one of which is within the Walker B motif (Tyr-569). Phosphorylation at Tyr-569 might be expected to interfere with ATP binding to the Walker sequences, which may explain the effects of src on the ATP-dependent low-frequency Lorentzian.

Although our data suggest a tyrosine phosphorylation may be regulating CFTR's gating, previous reports failed to find phosphotyrosines in biochemical assays (Cheng et al., 1991; Picciotto et al., 1992). It is therefore possible that tyrosine phosphorylation is only indirectly responsible for the high-frequency Lorentzian, and that it may initiate an interaction of CFTR with another cellular factor. This report, therefore, cannot specify a structural mechanism to relate tyrosine phosphorylation to gating. However, our data indicate that tyrosine phosphorylation affects a significant part of CFTR's gating. It also needs to be determined whether tyrosine phosphorylation itself is enough to activate the fast gate or if a blocking anion takes part in the rapid gating.

Previously we showed that the tyrosine kinase inhibitor genistein readily activated CFTR in a variety of cell types (Illek et al., 1995, 1996). All effects of genistein on CFTR were typical for blocking a serine phosphatase, i.e., (1) stimulation of silent CFTR in intact cells, (2) further stimulation of active CFTR at apparently saturated cAMP levels, and (3) inhibition of CFTR inactivation after agonist re

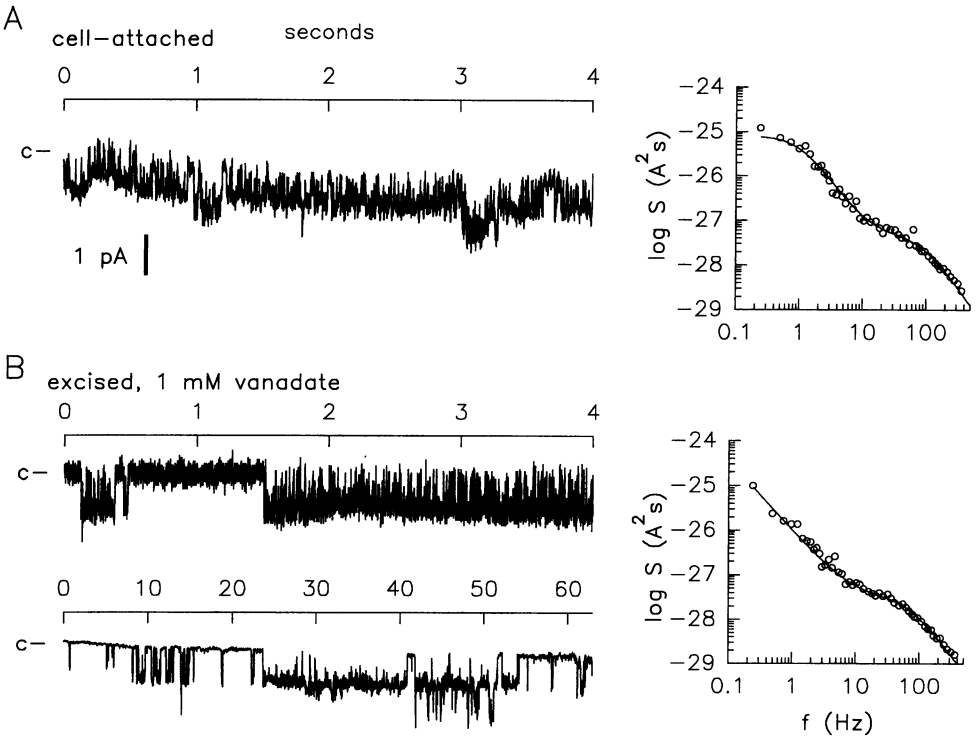

FIGURE 11 Effects of CFTR excision into vanadate. (*A*) Current recording from forskolin-stimulated 3T3 cell in the cell-attached mode and corresponding current noise spectrum (*right panel*). Fitted parameters were (f_{cl}, f_{ch}, S_{0l}, S_{0h}) 1.0 Hz, 81.1 Hz, 8.0E-26 A^2s, 4.8E-28 A^2s. (*B*) Recording after excision into 1 mM sodium vanadate. *Top panel* shows detail (at 21 s) of condensed *bottom panel* (sampled at 20 Hz). Current noise spectrum (*right panel*) was generated from the long open burst (from 20 s to 60 s). Fitted parameters were f_{ch} = 138 Hz, S_{0h} = 3.0E-28 A^2s. A linear background was fitted to low-frequency data. V_m = −77 mV. All *x*-axes of current traces are in seconds. c denotes all-closed level.

moval. Also, the kinetics of genistein-activated CFTR were indistinguishable from forskolin-stimulated CFTR (Fischer and Machen, 1994b). None of these characteristics was compatible with the observations presented in this report, indicating that genistein's effects on CFTR were not directly mediated by a src-like kinase.

We thank Dr. Willy Van Driessche, Leuven, Belgium, for continuing software support.

This study was supported by the Cystic Fibrosis Foundation and Cystic Fibrosis Research Inc.

REFERENCES

Akabas, M. H., C. Kaufmann, T. A. Cook, and P. Archdeacon. 1994. Amino acid residues lining the chloride channel of the cystic fibrosis transmembrane conductance regulator. *J. Biol. Chem.* 269: 14865–14868.

Anderson, M. P., R. J. Gregory, S. Thompson, D. C. Souza, S. Paul, R. C. Mulligan, A. E. Smith, and M. J. Welsh. 1991. Demonstration that CFTR is a chloride channel by alteration of its anion selectivity. *Science.* 253:202–205.

Baukrowitz, T., T. C. Hwang, A. C. Nairn, and D. C. Gadsby. 1995. Coupling of CFTR Cl channel gating to an ATP hydrolysis cycle. *Neuron.* 12:473–482.

Bischof, G., B. Illek, W. W. Reenstra, and T. E. Machen. 1995. Role of tyrosine kinases in carbachol-regulated Ca entry into colonic epithelial cells. *Am. J. Physiol.* 268:C154–C161.

Brautigan, D. L., and C. L. Shriner. 1988. Methods to distinguish various types of protein phosphatase activity. *Methods Enzymol.* 159:339–346.

Cantley, L. C., K. R. Auger, C. Carpenter, B. Duckworth, A. Graziani, R. Kapeller, and S. Solthoff. 1991. Oncogenes and signal transduction. *Cell.* 64:281–302.

Cheng, S. H., D. P. Rich, J. Marshall, R. J. Gregory, M. J. Welsh, and A. E. Smith. 1991. Phosphorylation of the R domain by cAMP-dependent protein kinase regulates the CFTR chloride channel. *Cell.* 66: 1027–1036.

Fischer, E. H., H. Charbonneau, and N. K. Tonks. 1991. Protein tyrosine phosphatases: a diverse family of intracellular and transmembrane enzymes. *Science.* 253:401–406.

Fischer, H., B. Illek, and T. E. Machen. 1994. Single channel characteristics of the genistein stimulated CFTR. *Mol. Biol. Cell* 5 (Suppl.):319a.

Fischer, H., and T. E. Machen. 1994a. CFTR displays voltage-dependence and two gating modes during stimulation. *J. Gen. Physiol.* 104:541–566.

Fischer, H., and T. E. Machen. 1994b. Activity of the CFTR is voltage-dependent in the cell-attached but not the excised patch clamp mode. *J. Gen. Physiol.* 104:37a (Abstr.)

Gray, M. A., A. Harris, L. Coleman, J. R. Greenwell, and B. E. Argent. 1989. Two types of Cl channel on duct cells cultured from human fetal pancreas. *Am. J. Physiol.* 257:C240–C251.

Gunderson, K. L., and R. R. Kopito. 1994. Effects of pyrophosphate and nucleotide analogues suggest a role for ATP hydrolysis in CFTR gating. *J. Biol. Chem.* 269:19349–19353.

Haws, C., W. E. Finkbeiner, J. H. Widdicombe, and J. J. Wine. 1994. CFTR in human airway cells: channel properties and role in cAMP-activated Cl conductance. *Am. J. Physiol.* 266:L502–L512.

Haws, C., M. E. Krouse, Y. Xia, D. C. Gruenert, and J. J. Wine. 1992. CFTR channels in immortalized human airway cells. *Am. J. Physiol.* 263:L692–L707.

Huganir, R. L., K. Miles, and P. Greengard. 1984. Phosphorylation of the nicotinic acetylcholine receptor by an endogenous tyrosine-specific protein kinase. *Proc. Natl. Acad. Sci. U. S. A.* 81:6968–6972.

Illek, B., H. Fischer, and T. E. Machen. 1996. Alternate regulation of apical CFTR by genistein in epithelia. *Am. J. Physiol.* 270:265–275.

Illek, B., H. Fischer, G. G. Santos, J. H. Widdicombe, T. E. Machen, and W. W. Reenstra. 1995. Cyclic-AMP independent activation of the CFTR Cl channel. *Am. J. Physiol.* 268:886–893.

Lee, K. M., K. Toscas, and M. L. Villereal. 1993. Inhibition of bradikinin and thapsigargin induced Ca entry by tyrosine kinase inhibitors. *J. Biol. Chem.* 268:9945–9948.

Matsumoto, P. S., A. Ohara, P. Duchatelle, and D. C. Eaton. 1993. Tyrosine kinase regulates epithelial sodium transport in A6 cells. *Am. J. Physiol.* 264:C246–C250.

McCarty, N. A., S. McDonough, B. N. Cohen, J. R. Riordan, N. Davidson, and H. A. Lester. 1993. Voltage-dependent block of the CFTR Cl channel by two closely related arylaminobenzoates. *J. Gen. Physiol.* 102:1–23.

Overholt, J. L., M. E. Hobart, and R. D. Harvey. 1993. On the mechanism of rectification of the isoproterenol-activated Cl current in guinea pig ventricular myocytes. *J. Gen. Physiol.* 102:871–895.

Picciotto, M., J. A. Cohn, G. Bertuzzi, P. Greengard, and A. C. Nairn. 1992. Phosphorylation of the cystic fibrosis transmembrane conductance regulator. *J. Biol. Chem.* 267:12742–12752.

Schultz, B. D., C. J. Venglarik, R. J. Bridges, and R. A. Frizzell. 1995. Regulation of CFTR Cl channel gating by ADP and ATP analogues. *J. Gen. Physiol.* 105:329–361.

Songyang, Z., K. L. Carraway III, M. J. Eck, S. C. Harrison, R. A. Feldman, M. Mohammadi, J. Schlessinger, S. R. Hubbard, D. P. Smith, C. Eng, M. J. Lorenzo, B. A. J. Ponder, B. J. Mayer, and L. C. Cantley. 1995. Catalytic specificity of protein tyrosine kinases is critical for selective signalling. *Nature.* 373:536–539.

Tabcharani, J. A., X. B. Chang, J. R. Riordan, and J. W. Hanrahan. 1991. Phosphorylation-regulated Cl channel in CHO cells stably expressing the CF gene. *Nature.* 352:628–631.

Tsui, L. C. 1992. The spectrum of cystic fibrosis mutations. *Trends Genet.* 8:392–398.

Venglarik, C. J., B. D. Schultz, R. A. Frizzell, and R. J. Bridges. 1994. ATP alters current fluctuations of CFTR: evidence for a three state gating mechanism. *J. Gen. Physiol.* 104:123–146.

Wilson, G. F., and L. K. Kaczmarek. 1993. Mode switching of a voltage gated cation channel is mediated by a protein kinase A regulated tyrosine phosphatase. *Nature.* 366:433–438.